Med Biol Eng Comput (2009) 47:1083–1091
DOI 10.1007/s11517-009-0529-x

ORIGINAL ARTICLE

On the EEG/MEG forward problem solution for distributed cortical sources

Nicolás von Ellenrieder · Pedro A. Valdés-Hernández · Carlos H. Muravchik

Received: 10 February 2009 / Accepted: 14 August 2009 / Published online: 4 September 2009

Abstract In studies of EEG/MEG problems involving cortical sources, the cortex may be modeled by a 2-D manifold inside the brain. In such cases the primary or impressed current density over this manifold is usually approximated by a set of dipolar sources located at the vertices of the cortical surface tessellation. In this study, we analyze the different errors induced by this approximation on the EEG/MEG forward problem. Our results show that in order to obtain more accurate solutions of the forward problems with the multiple dipoles approximation, the moments of the dipoles should be weighted by the area of the surrounding triangles, or using an alternative approximation of the primary current as a constant or linearly varying current density over plane triangular elements of the cortical surface tessellation. This should be taken into account when computing the lead field matrix for solving the EEG/MEG inverse problem in brain imaging methods.

Keywords EEG · MEG · Forward problem · Boundary element method · Cortical sources

1 Introduction

The EEG/MEG inverse problem is ill-conditioned, thus it is important to include any prior knowledge of the source of electric activity in the formulation of the problem [30]. When the significant brain activity is restricted to the brain cortex, this constraint is easily taken into account by assuming that all feasible sources are located in the gray matter. Since the cortical layer is a highly folded thin sheet with a columnar organization of pyramidal cells [17], it can be modeled as a bi-dimensional manifold. Then, the primary or impressed current density is restricted to this manifold, with a direction normal to the cortical surface [1]. The cortical surface is usually extracted from Magnetic Resonance (MR) images [2, 31], and described by a tessellation in plane triangular elements. The primary current is usually approximated by the combination of dipolar sources located at the vertices of the tessellation elements [1]. Even with this restriction, the ill-posedness of the inverse problem remains, and to deal with it some methods resort either to parametric sources models (small fixed number of dipoles [19], multipoles [15], or other parametric distributed sources [32]), or to "brain imaging" methods for which the inverse problem amounts to estimating the scalar distribution of the strength of the dipoles over the cortical surface. These latter methods usually deal with the ill-posedness by imposing some kind of smoothness to the inverse problem solution [10, 22]. Therefore, the sources of interest in brain imaging are usually distributed sources.

The tessellation of the cortical surface and subsequent approximation of the primary current density as a set of dipoles has some possible issues that we analyze in this study. First, the tessellation of the cortical surface should be sufficiently fine when compared to the source extent, in such a way that the set of dipoles on its vertices is an adequate approximation of the distributed source. Also, the normal direction to the tessellated surface is not uniquely defined on the vertices. It can be obtained by averaging the normal direction of the plane triangles around each vertex, but different averaging techniques yield different results.

N. von Ellenrieder (✉) · C. H. Muravchik
LEICI, Facultad de Ingeniería, Universidad Nacional de La Plata, Calle 1 y 47, B1900TAG La Plata, Argentina
e-mail: nellen@ieee.org

P. A. Valdés-Hernández
Centro de Neurociencias de Cuba, Havana, Cuba

Again, if the tessellation of the cortical surface is fine enough, it is expected that the elements around any vertex will have a similar normal direction, and any averaging technique will produce almost the same normal at the vertex. Another option would be to estimate the normal directions at the vertices from the MR images when extracting the cortical surface.

Since each dipole represents in some sense the effect of the surrounding elements, and usually the cortical surface tessellation does not have all its elements of the same size, the strength of the dipoles should somehow consider this. In [15], the authors weigh the strength of the dipoles by the "surface area they represent" when solving the MEG forward problem for a realistic cortical source, and claim that this "further enhances the realism of the patch model", but no comparison is made with the unweighted approximation. In this study, we quantify the difference between these approximations, and also show an alternative approximation for the primary current density as a constant or linearly varying current density over the plane triangles of the cortical surface tessellation. We show that the electric potential and magnetic field generated by these current density distributions can be computed analytically for a homogeneous and infinite media, and thus it can be incorporated in the integral formulation of the EEG/MEG forward problems, and used when solving it with the Boundary Element Method (BEM).

2 Materials and methods

In this section, we present EEG/MEG model assumptions and describe several approaches for handling distributed sources on the cortex in the forward problem. We also show that the electric potential and magnetic field generated by a 2-D patch of constant or linearly varying current density can be computed analytically, and describe the particular head model used to test the proposed methodologies.

2.1 Model assumptions

The head is modeled as a realistically shaped body with nested layers representing different tissues. The electric conductivity of each layer is assumed constant and isotropic. The head model is given then by the M surfaces S_1 to S_M, that are the interfaces between these constant conductivity layers, which in turn have electric conductivities σ_1 to σ_M, and defining $\sigma_{M+1} = 0$ as the conductivity outside the head.

The source of electric activity is a primary or impressed current density $\boldsymbol{J}_0(\boldsymbol{x})$, assumed to be restricted to the brain cortex, which is modeled as a surface S_c inside the brain volume Ω. The direction of this impressed current density is constrained to be normal to the cortical surface.

2.2 Electric potential

In this section, we analyze how to compute the electric potential generated by the sources in the adopted model. First, we describe existing approximations of distributed cortical sources as discrete sets of dipoles. These approximations are found in the literature, but to our knowledge there is no study comparing their performance. Then, we propose a new approximation of distributed cortical sources as dipolar sheets of current density over a tessellation of the cortical surface in plane triangular elements.

The integral formulation of the EEG forward problem [8], for any point $\boldsymbol{x} \in S_k$, $k = 1,...M$, is given by

$$\frac{(\sigma_{k+1}+\sigma_k)}{2}\phi(\boldsymbol{x}) = \phi_F(\boldsymbol{x}) + \frac{1}{4\pi}\sum_{m=1}^{M}(\sigma_{m+1}-\sigma_m) \int_{S_m} \phi(\boldsymbol{y})\nabla\left(\frac{1}{r}\right)\cdot\boldsymbol{n}(\boldsymbol{y})\mathrm{d}s(\boldsymbol{y}), \tag{1}$$

where $\phi(\cdot)$ is the electric potential, $\boldsymbol{n}(\cdot)$ is the unit vector normal to the surfaces S_m, $\mathrm{d}s(\boldsymbol{y})$ is the 2D surface area differential, with $\boldsymbol{y} \in S_m$, $r = |\boldsymbol{x}-\boldsymbol{y}|$, and the gradient is computed with respect to $\boldsymbol{y}$. The term $\phi_F(\boldsymbol{x})$ depends on the source of electric activity, i.e., the impressed or primary current density. It is the electric potential that would be generated by this source in an infinite and homogeneous media of unit conductivity. This term, for a known impressed current density $\boldsymbol{J}_0(\boldsymbol{y})$, with $\boldsymbol{x} \in \mathbb{R}^3$ and $\boldsymbol{y} \in \Omega$, is given by

$$\phi_F(\boldsymbol{x}) = \frac{1}{4\pi}\int_{\Omega}\boldsymbol{J}_0(\boldsymbol{y})\cdot\nabla\left(\frac{1}{|\boldsymbol{x}-\boldsymbol{y}|}\right)\mathrm{d}^3y. \tag{2}$$

If the source of electric activity is modeled as a dipole [5] at position $\boldsymbol{p}$ and with dipole moment $\boldsymbol{q}$, we have $\boldsymbol{J}_0(\boldsymbol{x}) = \boldsymbol{q}\boldsymbol{\delta}(\boldsymbol{x}-\boldsymbol{p})$, where $\boldsymbol{\delta}(\cdot)$ is a Dirac delta in three dimensional space, and

$$\phi_F(\boldsymbol{x}) = \frac{1}{4\pi|\boldsymbol{x}-\boldsymbol{p}|^3}\boldsymbol{q}\cdot(\boldsymbol{x}-\boldsymbol{p}). \tag{3}$$

When the source of electric activity is modeled as a surface current density restricted to the cortical surface S_c, usually the surface is tesselated in a set of plane triangles, and the surface current density is replaced by a set of dipolar sources located at the nodes or vertices of these triangles [13, 15], i.e.,

$$\boldsymbol{J}_0(\boldsymbol{y}) \approx \sum_{i=1}^{N_v} q_i\boldsymbol{n}(\boldsymbol{p}_i)\boldsymbol{\delta}(\boldsymbol{y}-\boldsymbol{p}_i), \tag{4}$$

and the resulting electric potential approximation is

$$\phi_F(\boldsymbol{x}) \approx \frac{1}{4\pi}\sum_{i=1}^{N_v} q_i\frac{\boldsymbol{n}_i\cdot(\boldsymbol{x}-\boldsymbol{p}_i)}{|\boldsymbol{x}-\boldsymbol{p}_i|^3}, \tag{5}$$

where $\boldsymbol{n}_i = \boldsymbol{n}(\boldsymbol{p}_i)$ is the unitary vector normal to the cortical surface at nodes $\boldsymbol{p}_i$.

Several approaches can be taken to choose the values of the discrete set of dipolar moments q_i, used to approximate the continuous dipolar sheet of current density. A simple one, usually found in the literature [13], which we will call Unweighted Multiple Dipoles (UMD) approximation, is to adopt

$$q_i = a\, J(\boldsymbol{p}_i), \quad i = 1, \ldots, N_v, \tag{6}$$

where the constant a can be chosen as to obtain any desired normalization (i.e., to choose the 1-norm or 2-norm of the primary current distribution). This approach gives equal weight to all the vertices $\boldsymbol{p}_i$ of the cortical surface. If the elements of the surface tessellation do not have an approximately equal size this may not be a good idea.

Another approximation, also found in the literature [15], which we will call Weighted Multiple Dipoles (WMD), takes into account the possibly different size in the elements of the cortical surface tessellation. We assume that these elements are triangular, and set

$$q_i = b\, J(\boldsymbol{p}_i) \sum_{l=1}^{N_i} \int_{\triangle_i^l} f_i(\boldsymbol{y}) \mathrm{d}s(\boldsymbol{y}), \tag{7}$$

where b is a normalization constant, N_i is the number of triangles sharing vertex $\boldsymbol{p}_i$, and $f_i(\boldsymbol{y})$ is a function varying linearly from a unit value on vertex $\boldsymbol{p}_i$ to a null value on the edges of the triangles $\triangle_i^l$ opposite to vertex $\boldsymbol{p}_i$, see Fig. 1. These integrals of $f_i(\boldsymbol{y})$ over the triangles can be computed analytically, yielding

$$\int_{\triangle_{ijk}} f_i(\boldsymbol{y}) \mathrm{d}s(\boldsymbol{y}) = \frac{d_{jk} h}{6}, \tag{8}$$

where we indicate explicitly the vertices of $\triangle_i^l$ by writing $\triangle_{ijk}$, d_{jk} is the distance between vertices $\boldsymbol{p}_j$ and $\boldsymbol{p}_k$, and h is the distance between vertex $\boldsymbol{p}_i$ and the line containing the other two vertices ($\boldsymbol{p}_j$ and $\boldsymbol{p}_k$). Note that this value is proportional to the area $d_{jk}\ h\ /2$ of the triangles, and then (7) is equivalent to

$$q_i = b_i\, J(\boldsymbol{p}_i), \tag{9}$$

where the weights b_i are proportional to the sum of the area of the triangles sharing vertex $\boldsymbol{p}_i$.

The multiple dipoles approximation of the source's current density (4) also depends on the normal vector $\boldsymbol{n}_i$ at the vertices of the cortical surface tessellation. Ideally, these directions should be obtained from the magnetic resonance images by the same methods used to obtain the cortical surface. Otherwise, they will not be uniquely defined and different approaches can be taken to compute them [18]. We will assume that only the surface

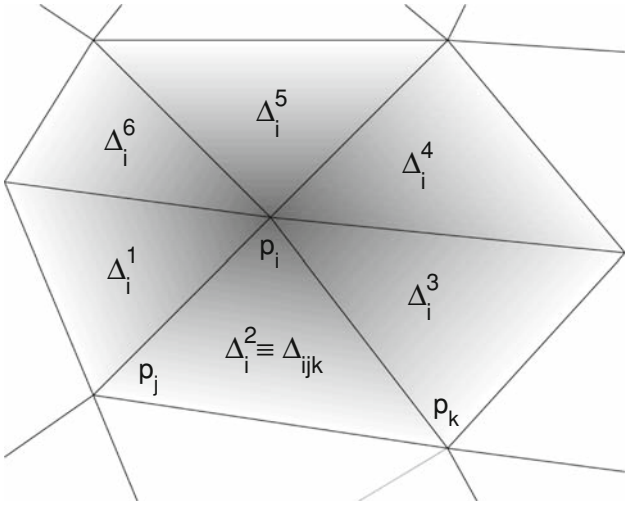

Fig. 1 Schematic representation of part of the cortical surface tessellation. The *triangles* $\triangle_i^l, l = 1, \ldots N_i{=}6$, surround node $\boldsymbol{p}_i$. A *triangle* can also be denoted by the indices of its vertices, e.g., $\triangle_{ijk}$ is formed joining the nodes $\boldsymbol{p}_i$, $\boldsymbol{p}_j$, and $\boldsymbol{p}_k$. The *gray tone* depicts a linear variation proportional to the function f_i in (7) and (18)

tessellation is known and test two different sets of normal vectors. We call the first of them Angle Average Normals, and obtain the normal vectors as

$$\boldsymbol{n}_i = a \sum_{l=1}^{N_i} \boldsymbol{\eta}_l \arccos\left(\frac{(\boldsymbol{p}_j - \boldsymbol{p}_i) \cdot (\boldsymbol{p}_k - \boldsymbol{p}_i)}{|\boldsymbol{p}_j - \boldsymbol{p}_i||\boldsymbol{p}_k - \boldsymbol{p}_i|} \right), \tag{10}$$

where a is a constant chosen as to obtain a unit norm for the normal vector, $\boldsymbol{\eta}_l$ is the unit vector normal to the plane triangle $\triangle_i^l$ with vertices $\boldsymbol{p}_i$, $\boldsymbol{p}_j$, and $\boldsymbol{p}_k$. The normal direction $\boldsymbol{\eta}_l$ to the plane triangle $\triangle_{ijk}$ is easily obtained as

$$\boldsymbol{\eta}_l = \pm \frac{(\boldsymbol{p}_j - \boldsymbol{p}_i) \times (\boldsymbol{p}_k - \boldsymbol{p}_i)}{|(\boldsymbol{p}_j - \boldsymbol{p}_i) \times (\boldsymbol{p}_k - \boldsymbol{p}_i)|}, \tag{11}$$

where in our case the sign is chosen as to obtain an outward pointing normal direction.

Another possibility is to compute what we will call the Area Average Normals, computed as an average of the normal vectors of the triangles, with a linear weighing function $f_i(\boldsymbol{y})$ over the triangles sharing vertex $\boldsymbol{p}_i$, i.e.,

$$\boldsymbol{n}_i = b \sum_{l=1}^{N_i} \boldsymbol{\eta}_l \int_{\triangle_i^l} f_i(\boldsymbol{y}) \mathrm{d}s(\boldsymbol{y}) = \sum_{l=1}^{N_i} b_l\, \boldsymbol{\eta}_l. \tag{12}$$

Once again this is equivalent to a weighted average of the normal vectors of triangles sharing vertex $\boldsymbol{p}_i$, with the weights b_l proportional to the area of the surrounding triangles. The approach described in this paragraph is how the direction of the *VertexNormal* property of MATLAB® `patch` structures is computed.

Next, we propose a new approach for computing the source term (15) of the EEG forward problem. The smooth

surface S_c can be defined as a level set of a smooth function $g(\boldsymbol{x})$, e.g., $S_c = \{\boldsymbol{x}: g(\boldsymbol{x}) = 0\}$. Let us assume also that $|\nabla g(\boldsymbol{x})| = 1, \forall \boldsymbol{x} \in S_c$. Then, a model of the source of electric activity as a surface current density restricted to the cortical surface S_c, with direction normal to the surface, and intensity $J_0(\boldsymbol{y})$, $\boldsymbol{y} \in S_c$, can be expressed as

$$\boldsymbol{J}_0(\boldsymbol{x}) = J_0(\boldsymbol{y})\boldsymbol{n}(\boldsymbol{y})\boldsymbol{\delta}(g(\boldsymbol{x})), \qquad \boldsymbol{y} \in S_c, \tag{13}$$

i.e., the surface current density is zero in any point $\boldsymbol{x}$ not belonging to S_c, and is a dipole with intensity J_0 and orientation $\boldsymbol{n}$ for any point belonging to this cortical surface. Thus, it is modeled as a dipolar sheet of volume current density. Replacing (13) in (2), we get a simple layer integral, and using the identity [12, sec.6.1],

$$\int_{\mathbb{R}^3} f(\boldsymbol{y})\delta(g(\boldsymbol{y}))\mathrm{d}^3 y = \int_{g^{-1}(0)} \frac{f(\boldsymbol{y})}{|\nabla g(\boldsymbol{y})|}\mathrm{d}s(\boldsymbol{y}), \tag{14}$$

where $f(\boldsymbol{y})$ is any smooth function, the electric potential in an infinite media results

$$\phi_F(\boldsymbol{x}) = \frac{1}{4\pi}\int_{S_c} J_0(\boldsymbol{y})\boldsymbol{n}(\boldsymbol{y}) \cdot \nabla\left(\frac{1}{|\boldsymbol{x}-\boldsymbol{y}|}\right)\mathrm{d}s(\boldsymbol{y}). \tag{15}$$

We propose to approximate this dipolar sheet of current density over the true cortical surface S_c by a similar dipolar sheet over the faceted cortical surface, with constant or linearly varying intensity over the plane triangles, i.e.,

$$\phi_F(\boldsymbol{x}) \approx \frac{1}{4\pi}\sum_{i=1}^{N_v} J(\boldsymbol{p}_i)\sum_{l=1}^{N_i}\int_{\triangle_i^l} f_i(\boldsymbol{y})\nabla\left(\frac{1}{|\boldsymbol{x}-\boldsymbol{y}|}\right)\cdot\boldsymbol{\eta}_l\mathrm{d}s(\boldsymbol{y}), \tag{16}$$

where N_v is the number of vertices of the cortical surface tessellation, N_i is the number of triangles $\triangle_i^l$ with $\boldsymbol{p}_i$ as one of its vertices, and the function $f_i(\boldsymbol{y})$ determines if the primary surface current density is approximated as a Piecewise Constant (PC) or Piecewise Linear (PL) function. For the PC approximation, we must adopt

$$f_i(\boldsymbol{y}) = \begin{cases} 1/3 & \boldsymbol{y} \in \triangle_i^l \\ 0 & \boldsymbol{y} \notin \triangle_i^l, \end{cases} \tag{17}$$

and for the PL approximation

$$f_i(\boldsymbol{y}) = \begin{cases} \frac{\boldsymbol{y}\cdot(\boldsymbol{p}_j\times\boldsymbol{p}_k)}{\boldsymbol{p}_i\cdot(\boldsymbol{p}_j\times\boldsymbol{p}_k)} & \boldsymbol{y} \in \triangle_i^l \\ 0 & \boldsymbol{y} \notin \triangle_i^l, \end{cases} \tag{18}$$

where again $\triangle_i^l$ is any of the triangles that has $\boldsymbol{p}_i$ as one of its vertices, and the remaining vertices are $\boldsymbol{p}_j$ and $\boldsymbol{p}_k$, see Fig. 1.

The integrals in (16) have the same form as the integrals in (1) when the surfaces are tesselated for solving the EEG forward problem with the BEM, and they can be evaluated analytically. In particular, for the PC approximation the value of $\int_{\triangle}\nabla(1/|\boldsymbol{x}-\boldsymbol{y}|)\cdot\boldsymbol{\eta}\mathrm{d}s(\boldsymbol{y})$ is given in [24]. An expression for the value of $\int_{\triangle_{ijk}} \boldsymbol{y}\cdot(\boldsymbol{p}_j\times\boldsymbol{p}_k)/(\boldsymbol{p}_i\cdot(\boldsymbol{p}_j\times\boldsymbol{p}_k))\nabla(1/|\boldsymbol{x}-\boldsymbol{y}|)\cdot\boldsymbol{\eta}\mathrm{d}s(\boldsymbol{y})$ for the PL approximation is given in [3]. Once these integrals are computed, the term $\Phi_F(\boldsymbol{x})$ in (1) can be evaluated at any point $\boldsymbol{x}$ as a linear combination of the primary current density values at the vertices of the cortical surface tessellation $J(\boldsymbol{p}_i)$.

2.3 Magnetic field

Once the electric potential is known, it is possible to solve the MEG forward problem, to obtain the magnetic field in any point $\boldsymbol{x}$ as [9]

$$\boldsymbol{B}(\boldsymbol{x}) = \boldsymbol{B}_F(\boldsymbol{x}) - \frac{\mu}{4\pi}\sum_{m=1}^{M}(\sigma_{m+1}-\sigma_m)\cdot\int_{S_m}\phi(\boldsymbol{y})\nabla\left(\frac{1}{r}\right)\times\boldsymbol{n}(\boldsymbol{y})\mathrm{d}s(\boldsymbol{y}), \tag{19}$$

where μ is the magnetic permeability of the non-magnetic tissues which will be considered equal to the magnetic permeability of vacuum μ_0, and $\boldsymbol{B}_F(\boldsymbol{x})$ is the magnetic field that would be generated by the primary current density in an infinite and homogeneous media. It is given by

$$\boldsymbol{B}_F(\boldsymbol{x}) = \frac{\mu_0}{4\pi}\int_{\Omega}\boldsymbol{J}_0(\boldsymbol{y})\times\nabla\left(\frac{1}{|\boldsymbol{x}-\boldsymbol{y}|}\right)\mathrm{d}^3 y. \tag{20}$$

With the approximations of the primary current $\boldsymbol{J}_0(\boldsymbol{x})$ given in the previous section, we get

$$\boldsymbol{B}_F(\boldsymbol{x}) \approx \frac{\mu_0}{4\pi}\sum_{i=1}^{N_v}\frac{\boldsymbol{q}_i\times(\boldsymbol{x}-\boldsymbol{p}_i)}{|\boldsymbol{x}-\boldsymbol{p}_i|^3}, \tag{21}$$

for the multiple dipole approximations (5), and

$$\boldsymbol{B}_F(\boldsymbol{x}) \approx \frac{\mu_0}{4\pi}\sum_{i=1}^{N_v} J(\boldsymbol{p}_i)\sum_{l=1}^{N_i}\int_{\triangle_i^l} f_i(\boldsymbol{y})\boldsymbol{\eta}_l\times\nabla\left(\frac{1}{|\boldsymbol{x}-\boldsymbol{y}|}\right)\mathrm{d}s(\boldsymbol{y}), \tag{22}$$

for the piecewise constant and linear approximations. Again, the integrals related to the PC and PL approximations are the same as the ones that appear in (19) when solving the MEG forward problem with the BEM. Analytical expressions for the value of $\int_{\triangle}\boldsymbol{\eta}\times\nabla(1/|\boldsymbol{x}-\boldsymbol{y}|)\mathrm{d}s(\boldsymbol{y})$ appear in [11], and for the value of $\int_{\triangle_{ijk}}\frac{\boldsymbol{y}\cdot(\boldsymbol{p}_j\times\boldsymbol{p}_k)}{\boldsymbol{p}_i\cdot(\boldsymbol{p}_j\times\boldsymbol{p}_k)}\boldsymbol{\eta}\times\nabla(\frac{1}{|\boldsymbol{x}-\boldsymbol{y}|})\mathrm{d}s(\boldsymbol{y})$, in [6].

2.4 Problem setup

In order to test the proposed approaches, we computed EEG and MEG forward problem simulations. The adopted head model corresponded to a subject of the Cuban Human Brain Mapping Project database, and consists of three surfaces delimiting the brain, skull, and scalp. The inner

surface of the model was tessellated in 10240 triangular elements, and the other two surfaces in 5120 triangular elements. The adopted tissue electric conductivity values were 0.3 S/m for the brain and scalp, and 0.02 S/m for the skull [21, 28, 33]. We solved the forward problem for 120 electrodes on the scalp, placed according to an extension of the 10–20 system [14], and 160 magnetometers on a helmet, with approximately radial orientation and about 2 cm away from the scalp surface. The forward problem was solved using the BEM, with linear elements [3] and the Isolated Problem Approach [18].

The cortical surface S_c was selected as the surface that passes through the middle of the gray matter. It was tessellated in 7201 plane triangular elements, see Fig. 2. As profile for the distributed sources we adopted a Gaussian shape, and the standard deviation of this Gaussian shape is what we call the source extent. All the distances over the cortical surface are measured using geodesic distance.

In order to compare the forward problem results, we used the Normalized Relative Difference Measure (NRDM) [18], given by

$$\mathrm{NRDM} = \left\| \frac{\boldsymbol{v}_a}{\| \boldsymbol{v}_a \|} - \frac{\boldsymbol{v}_b}{\| \boldsymbol{v}_b \|} \right\|, \tag{23}$$

where $\boldsymbol{v}_a$ and $\boldsymbol{v}_b$ are the forward problem solutions computed with different approaches, and all the norms are 2-norms. This choice of difference measures produce results that are independent of the choice of normalization adopted in (6) and (7).

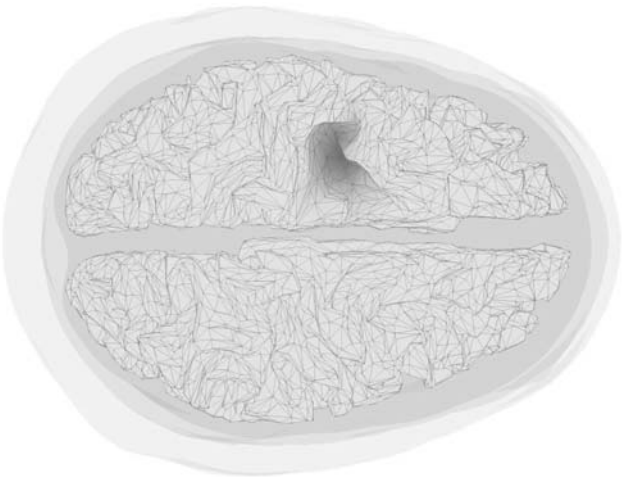

Fig. 2 Head model used in the study. The surfaces delimiting brian, skull, and scalp are shown in shades of *gray*. The cortical surface tessellation is shown, with one distributed source with Gaussian profile and 10 mm extent (i.e., 10 mm standard deviation). The *gray tone* is proportional to intensity of the imposed current density

3 Results

In this section, we present some simulation results. First, a simple source geometry is used to show that the Unweighted Multiple Dipoles approximation of the source produces results that do not converge to the same value as the rest of the approximations when the cortical surface tessellation is refined. Then, we compare the performance of the proposed approximations for sources on a realistically shaped cortical surface. The EEG and MEG forward problem performance is analyzed as a function of the source extent. We find a coarse estimate of the average relationship between source extent and size of the elements of the cortical surface tessellation, needed to obtain forward problem results of good accuracy. Given the realistic shape of the head model, it is impossible to obtain an analytic solution of the forward problem. Then, the shown results are not absolute errors, but comparisons among the tested approximations, choosing one of them as the reference.

First, we test the proposed approximations of the distributed source in the EEG forward problem. The source has a Gaussian profile, with an extent, i.e., standard deviation, of 8 mm. It is located in a plane surface inside the brain, tessellated in equilateral triangles of fixed edge lengths of 6, 3, 1.5, and 0.75 mm. The plane is parallel to the plane defined by the nasion and the preauricular points, 48 mm above it. The source is centered exactly above the midpoint between the preauricular points. In this situation all the proposed approaches should converge to the same value for finer tessellations, and this is indeed the case, as shown in Fig. 3 (lines with white markers). In the figure, all the approaches are compared to the PL approximation of the impressed current density, i.e., the PL approximation is chosen as the reference. Since all the triangular elements are of the same size, there is no difference between the UMD and WMD approximations in this case. Also, the true normal direction is known in all the vertices. All the approaches exhibit the same quadratic convergence rate.

We analyze also a second situation where the vertices of the surface tessellation are displaced slightly on the plane to produce a 10% random variation in the edge lengths. The same source in the plane surface is considered. The results are also shown in Fig. 3 (lines with black markers). As expected, now the UMD approximation does not converge to the same value as the other approaches. It is important to note that the variation of the edge lengths is set in the initial tessellation, and the finer tessellations are obtained from the original one by halving the length of the edges, without further modifications. This example shows that the Unweighted Multiple Dipoles approximation cannot be expected to converge to the true solution of the forward problem as the tessellation gets smaller, assuming

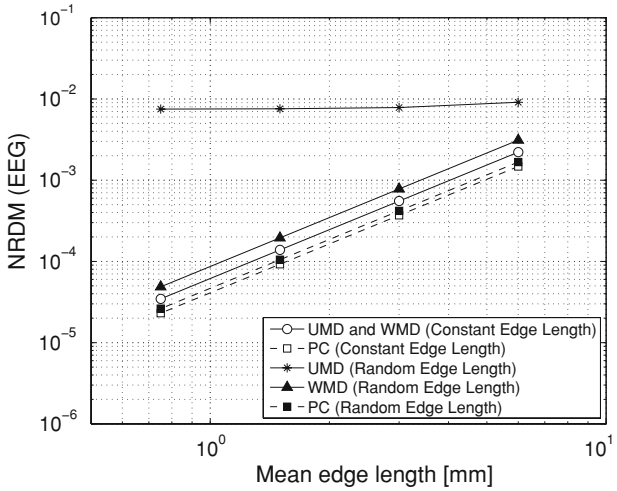

Fig. 3 Comparison of the EEG forward problem solution for different approximations of the primary current density, for a distributed source of Gaussian shape on a plane surface inside the brain. The surface was tesselated with triangles of constant edge length and of variable edge length. NRDM of the Weighted and Unweighted Multiple Dipoles approximations, and the Piecewise Constant approximation of the source distribution compared to the Piecewise Linear approximation results

that the true solution is the one to which the WMD, PC, and PL approximations converge. These latter approaches show the same convergence rate as for constant edge length, with a slight increment of the NRDM value. The results for the MEG forward problem are not shown, but are similar to the EEG results, so the same conclusion holds: the refinement of the Cortex tessellation does not guarantee convergence to the true forward problem solution if the UMD approximation is adopted.

The remaining results are obtained for distributed sources on the realistically shaped cortical surface described in the previous section. We compare the different approximations of the source and study the error in the forward problem as a function of the source extent. In this case the mean edge length of the triangular elements of the surface tessellation is 5 mm, and its standard deviation 2.3 mm, so the variation in the edge length is much higher than in the previous case, and we expect a larger difference between the UMD approximation and the other approaches. The cortex tessellation we use is the surface provided by the SPM8b (Statistical Parametric Mapping) toolbox [7, 27], adapted to the shape of the subject. A similar variability in the length of the vertices is found in earlier surfaces from earlier versions of the toolbox, e.g. SPM5.

Also, the normal direction in the vertices is not uniquely determined, and the Angle Average Normals and Area Average Normals differ in a mean value of 8.2°, with a standard deviation of 6.8°. Hence, both approaches should produce different results. This is confirmed by the EEG forward problem results shown in Fig. 4 and the MEG forward problem results shown in Fig. 5. The figures show the mean value of the forward problem error for 100 sources with randomly selected positions, uniformly distributed on the cortical surface. The NRDM is shown as a function of the extent of the sources. The reference with which all the approaches are compared is the result of the forward problem computed with the WMD approximation and a cortical surface in which every triangle of the original surface is divided into 16 smaller triangles, with a mean edge length of 1.3 mm. The results do not vary significantly if PC or PL approximation results on this finer surface tessellation are used as the reference.

The UMD approach has a small error when the source extent is significantly smaller than the cortical surface tessellation, since in this case a good approximation is to assume that the source is a single dipole. For sources of the same size as the surface tessellation for EEG, or twice this size for MEG, the UMD approximation has a maximum error because in this case the approximation of a Gaussian source with dipoles is not very good. For sources much larger than the surface tessellation, the error decreases again, but stabilizing in a value of NRDM between 0.1 and 0.15.

The results of the Multiple Dipoles approximations also seem to have a large sensitivity to the selected normal directions on the vertices. Figures 4 and 5 also show that the Area Average Normals produce results that are closer to the PC and PL approximation results, both for EEG and

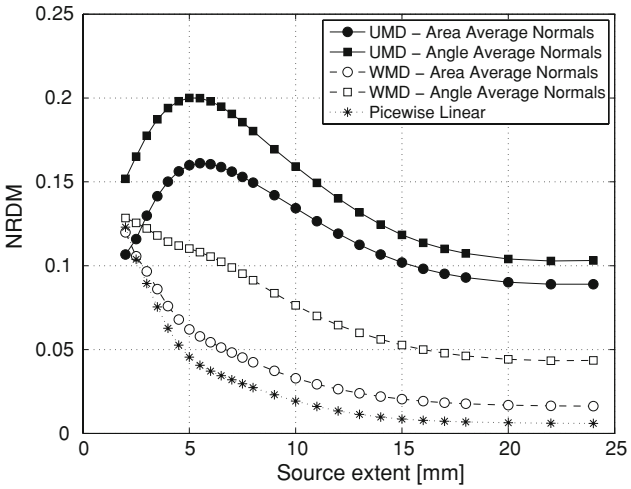

Fig. 4 Mean NRDM error of the EEG forward problem solution for different approximations of the primary current density, for 100 distributed sources of Gaussian shape on the cortical surface. The results are shown for Weighted and Unweighted Multiple Dipoles approximations for the source term with the normal vectors in the vertices computed as Angle Averages and Area Average of the normals to the *triangles* around each vertex. The results for the Piecewise Linear approximation of the source term is also shown

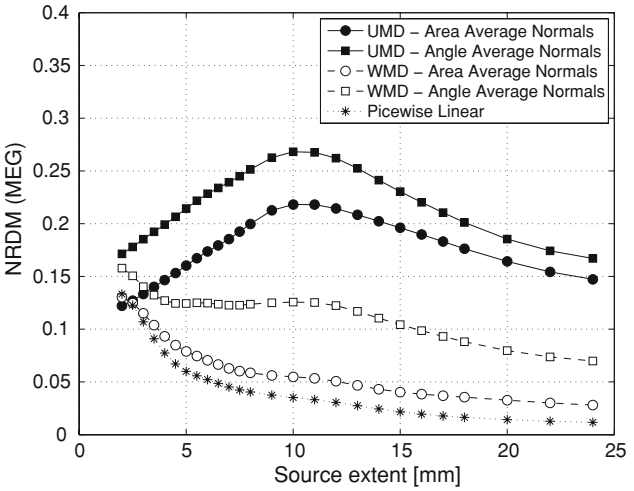

Fig. 5 Mean NRDM error of the MEG forward problem solution for different approximations of the primary current density, for 100 distributed sources of Gaussian shape on the cortical surface. The results are shown for Weighted and Unweighted Multiple Dipoles approximations for the source term with the normal vectors in the vertices computed as Angle Averages and Area Average of the normals to the *triangles* around each vertex. The results for the Piecewise Linear approximation of the source term is also shown

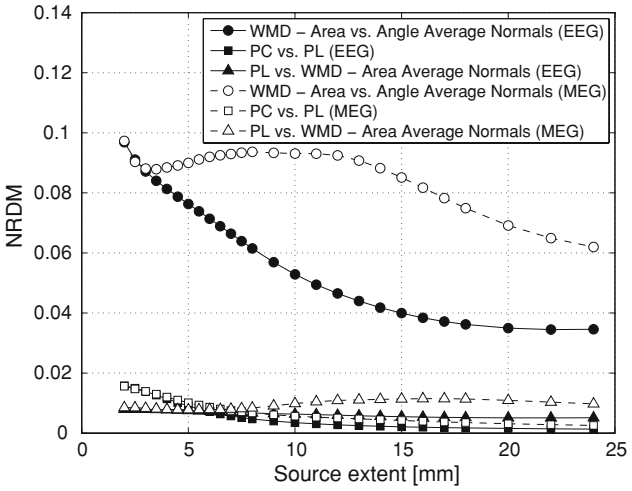

Fig. 6 Comparison between the EEG and MEG forward problem solutions for different approximations of the primary current density. Mean behavior for 100 distributed sources of Gaussian shape on the cortical surface. For the Weighted Multiple Dipoles (WMD) approximation the difference between two approaches for computing the Normal directions on the vertices is shown. The figure also shows the difference between the results of the Piecewise Constant (PC) approximation and the Piecewise Linear (PL) one. Also shown is the difference between the WMD approximation and the PL approximation in a finer surface tessellation with 16 times more *triangles*

MEG forward problems. In addition, we can note in these figures that the PL approximation produces the best results, although not too different from the WMD approximation. The results of the PC approximation are omitted in these figures for clarity, since they are almost equal to the results of the PL approximation.

In order to confirm the assertions made in the previous paragraphs, we show some more results in Fig. 6. The figure shows a comparison of the results obtained using the WMD approximation with Angle Average and Area Average Normals, both for EEG and MEG. We observe that the difference is higher for MEG, reaching a NRDM of almost 0.1, than for EEG, for which the NRDM is below 0.05 for sources larger than twice the mean edge length. We also show in this figure that the difference between PL and PC approximations is small for EEG and MEG, and the difference between WMD and PL approximations is also small, below 0.01, for the finer surface tessellation.

It is important to note that the results shown in the previous paragraphs correspond to average values of the NRDM errors, computed from 100 sources at different positions on the cortical surface. The dispersion around the shown average values may have several causes; a study of probable causes is not carried out in this study. Such a study would be useful in pointing strategies that could be used to adaptively refine the cortical surface tessellation. It is possible, e.g., that an efficient tessellation would not have a uniform edge length, but finer tessellations in regions with more curvature.

4 Discussion

When solving the EEG/MEG forward problem the errors or approximations can be separated into two groups; one kind of errors is related to the difference between the model and the reality, i.e., modeling errors, and the other kind to errors or approximations made when solving the problem, e.g., inaccuracies of the numerical algorithms for solving the differential or integral equations. For the modeling errors there is a tradeoff between accuracy and complexity; there are some simple head models, such as concentric spherical layers of constant electric conductivity, for which analytical solutions of the forward problem exist [4], and very detailed models including many tissues and anisotropic electric conductivity [23], which must be solved with numerical methods such as Finite Elements [29] or Finite Differences [20]. For the model adopted in this study, consisting of three realistically shaped layers of constant electric conductivity, several causes of errors have been analyzed in the literature, e.g., the numerical error associated to the BEM method [18, 3], errors in the assumed shape of the layers [25], or errors in the assumed sensor positions [26]. In this study, we analyzed the errors committed when a source modeled as a distributed source over the cortical surface is approximated by sets of dipoles or by dipolar sheets of current density over plane triangular elements. We present some general recommendations that can be derived from the results shown in the previous section.

The first conclusion is that the Unweighted Multiple Dipoles approximation of a distributed source is not a good approximation when the elements of the cortical surface tessellation are not of the same size, which is usually the case. In the example shown in the previous section, we got NRDM errors of up to 0.2. In order to have an idea of the magnitude of this error, consider that it is similar to the modeling error due to the isotropic conductivity assumption [29]. A refinement of the cortical surface tessellation does not necessarily reduce the error of the UMD approximation, since it is not related to the average size of the mesh elements but to the variance of their size. However, even if the cortical surface tessellation is homogenous enough as to consider the UMD approximation error acceptable from a practical point of view, it would still be wiser to use de WMD approximation, since it has lower error and almost the same computational load.

Another important issue for the Multiple Dipoles approximations (UMD and WMD) is the choice of normal direction at the vertices of the cortical surface tessellation. The studied normal directions obtained as weighted averages of the normals to the triangles surrounding a node produce results with NRDM up to 0.1. Several strategies could be used to deal with this problem. One possibility would be to obtain the normal directions from the MR image, with the same algorithm used to extract the cortical surface. Another possibility is to work with a finer tessellation than the one used in this study; this should lead to smaller differences between the Angle Average and Area Average Normals, and any other sensible methods for computing the normals [16]. A third option, not analyzed in this study, is to allow for a variable orientation of the surface current density, but this implies a much larger computational burden for solving the inverse problem. The Piecewise Constant and Linear approximations, which do not depend of the choice of normal directions at the vertices of the tessellation, give results similar to the Weighted Multiple Dipoles approach with Area Average Normals. This could be a reason to favor the Area Average Normals when the true normals are unknown.

The performance of the Area Average WMD and of the PC and PL approximation is similar; the error decreases as the ratio between source extent and element size of the surface tessellation increases. If we want to obtain results of the EEG and MEG forward problem with negligible errors due to the cortical surface tessellation when compared to other errors of the adopted model, we should aim to a NRDM value of 0.02. This value is approximately ten times smaller than the error due to the isotropy assumption for the electric conductivity of the tissues [29]. For the surface tessellation provided in the SPM8b toolbox, with 7201 vertices, this implies using Gaussian sources with standard deviation of at least 10 mm for EEG and 15 mm for MEG. This corresponds to a mean edge length of one half of the source extent for the EEG forward problem, and one third of the source extent for the MEG forward problem. For more concentrated sources, a finer tessellation would be needed to maintain the error level.

The Piecewise Constant and the Piecewise Linear approximations are marginally better than the Weighted Multiple Dipoles approximation, but also require more computational resources. A comparison between the Piecewise Linear and the Piecewise Constant approximations regarding the computational load, shows that for the linear approximation the computation for each node is more complex, but the number of nodes is only half as much as for the constant approximation (number of vertices compared to number of triangles). We found that the Piecewise Linear approach is about 30% faster in our implementation, considering only the time needed to assemble the lead field matrix once the BEM linear system has already been solved. This means that the difference is not very significant.

The effect of the studied approximations on the inverse problem will depend on the chosen algorithm, in brain imaging methods these approximations introduce errors in the lead field matrix. However, if the cortical mesh is fine enough, the Area Average Normals Weighted Multiple Dipoles approximation and the Piecewise approximations would produce solutions of the inverse problem with differences of no practical significance.

Acknowledgments This study was funded by ANPCyT PICT 11-00535 and PICT 35423, by the MinCyT (Argentina)—CITMA (Cuba) Bilateral Cooperation Project CU/PA/03–SV/022, and by UNLP. The study of NvE was supported by CONICET and that of CHM was supported by CICpBA.

References

1. Dale AM, Sereno MI (1993) Improved localizadon of cortical activity by combining EEG and MEG with MRI cortical surface reconstruction: a linear approach. J Cogn Neurosci 5(2):162–176. doi:10.1162/jocn.1993.5.2.162
2. Davatzikos C, Bryan N (1996) Using a deformable surface model to obtain a shape representation of the cortex. IEEE Trans Med Imag 15(6):785–795. doi:10.1109/42.544496
3. de Munck JC (1992) A linear discretization of the volume conductor boundary integral equation using analytically integrated elements. IEEE Trans Biomed Eng 39(9):986–990
4. de Munck JC, Peters MJ (1993) A fast method to compute surface potentials in the multisphere model. IEEE Trans Biomed Eng 40(11):1166–1174
5. de Munck JC, Vijn PCM, Lopes da Silva FH (1992) A random dipole model for spontaneous brain activity. IEEE Trans Biomed Eng 39(8):791–804
6. Ferguson AS, Zhang X, Stroink G (1994) A complete linear discretization for calculating the magnetic field using the boundary element method. IEEE Trans Biomed Eng 41(5): 455–460

7. Friston K, Ashburner J, Kiebel S, Nichols T, Penny W (eds) (2007) Statistical parametric mapping: the analysis of functional brain images. Academic Press, New York
8. Geselowitz DB (1967) On bioelectric potentials in an inhomogenous volume conductor. Biophys J 7:1–11
9. Geselowitz DB (1970) On the magnetic field generated outside an inhomogeneous volume conductor by internal current sources. IEEE Trans Magn MAG-6:346–347
10. Hämäläinen MS, Ilmoniemi RJ (1994) Interpreting magnetic fields of the brain: minimum norm estimates. Med Biol Eng Comput 32:35–42
11. Hämäläinen MS, Sarvas J (1989) Realistic conductivity geometry model of the human head for interpretation of neuromagnetic data. IEEE Trans Biomed Eng 36(2):165–171
12. Hörmander L (1990) The analysis of linear partial differential operators I: distribution theory and fourier analysis, 2nd edn. No. 256. In: Grundlehren der Mathematischen Wissenschaften, Springer, Berlin
13. Im CH, Gururajan A, Zhang N, Chenb W, He B (2007) Spatial resolution of EEG cortical source imaging revealed by localization of retinotopic organization in human primary visual cortex. J Neurosci Methods 16:142–154
14. Jasper H (1958) The ten twenty electrode system of the international federation. Electroencephalogr Clin Neurophysiol 10: 371–375
15. Jerbi K, Baillet S, Mosher JC, Nolte G, Garnero L, Leahy RM (2004) Localization of realistic cortical activity in MEG using current multipoles. NeuroImage 22(2):779–793
16. Lin FH, Belliveau JW, Dale AM, Hämäläinen MS (2006) Distributed current estimates using cortical orientation constraints. Human Brain Mapp 27(1):1–13
17. Malmivuo J, Plonsey R (1995) Bioelectromagnetism—principles and applications of bioelectric and biomagnetic fields. Oxford University Press, Oxford
18. Meijs JWH, Weier OW, Peters MJ, van Oosterom A (1989) On the numerical accuracy of the boundary element method. IEEE Trans Biomed Eng 36(10):1038–1049
19. Mosher JC, Leahy RM (1998) Recursive MUSIC: a framework for EEG and MEG source localization. IEEE Trans Biomed Eng 45(11):1342–1354
20. Neilson LA, Kovalyov M, Koles ZJ (2005) A computationally efficient method for accurately solving the EEG forward problem in a finely discretized head model. Comput Mech 116(10): 2302–2314
21. Oostendorp TF, Delbecke J, Stegeman DF (2000) The conductivity of the human skull: Results of in vivo and in vitro measurements. IEEE Trans Biomed Eng 47(11):1467–1492
22. Pascual-Marqui RD, Michel CM, Lehmann D (1994) Low resolution electromagnetic tomography: a new method for localizing electrical activity in the brain. Int J Psychophysiol 18:49–65
23. Tuch D, Wedeen V, Dale A, George J, Belliveau J (2001) Conductivity tensor mapping of the human brain using diffusion tensor MRI. Proc Natl Acad Sci USA 98:11,697–11,701
24. van Oosterom A, Strackee J (1983) The solid angle of a plane triangle. IEEE Trans Biomed Eng 30(2):125–126
25. von Ellenrieder N, Muravchik CH, Nehorai A (2006) Effects of geometric head model perturbations on the EEG inverse problem. IEEE Trans Biomed Eng 53(2):249–257
26. Wang Y, Gotman J (2001) The influence of electrode location errors on EEG dipole source localization with a realistic head model. Clin Neurophysiol 112:1777–1780
27. Wellcome Trust Center for Neuroimaging (2008) Statistic parametrical mapping (SPM) toolbox. Online, URL http://www.fil.ion.ucl.ac.uk/spm/
28. Wendel K, Malmivuo J (2006) Correlation between live and post mortem skull conductivity measurements. In Twenty-eighth annual international conference of the IEEE engineering in medicine and biology society, EMBS '06, pp 4285–4288. doi: 10.1109/IEMBS.2006.259434
29. Wolters CH, Anwander A, Tricoche X, Weinstein D, Koch MA, MacLeod RS (2006) Influence of tissue conductivity anisotropy on EEG/MEG field and return current computation in a realistic head model: a simulation and visualization study using high-resolution finite element modeling. NeuroImage 30(3):813–826
30. Wood CC, George JS, Lewis PS, Ranken DM, Heller L (1990) Anatomical constraints for neuromagnetic source models. Soc Neurosci, Abstracts 16:1241
31. Xu C, Pham D, Rettmann M, Yu D, Prince J (1999) Reconstruction of the human cerebral cortex from magnetic resonance images. IEEE Trans Med Imag 18(6):467–480
32. Yetik I, Nehorai A, Muravchik C, Haueisen J, Eiselt M (2006) Surface-source modeling and estimation using biomagnetic measurements. IEEE Trans Biomed Eng 53(10):1872–1882
33. Zhang Y, van Drongelen W, He B (2006) Estimation of in vivo brain-to-skull conductivity ratio in humans. Appl Phys Lett 89(22):223,903–2239,033